





















ORIGINAL RESEARCH



Peripheral memory B cell population maintenance and long-term survival after perioperative chemoimmunotherapy in NSCLC (NADIM trial)

Belén Sierra Rodero ^a, Cristina Martínez-Toledo ^a, Ernest Nadal ^b, Marta Molina-Alejandre ^a, Rosario García Campelo ^c, Ángeles Gil-González ^a, Bartomeu Massuti ^d, Aránzazu García-Grande ^e, Manuel Dómine ^f, Amelia Insa ^g, Javier de Castro Carpeño ^h, Gerardo Huidobro Vence ⁱ, Margarita Majem ^j, Alex Martínez-Martí ^k, Diego Megías ^l, Daniel Lobato ^a, Ana Collazo-Lorduy ^a, Virginia Calvo ^a, Mariano Provencio ^a, and Alberto Cruz-Bermúdez ^a

^aServicio de Oncología Médica, Instituto de Investigación Sanitaria Puerta de Hierro-Segovia de Arana (IDIPHISA), Hospital Universitario Puerta de Hierro-Majadahonda, Madrid, Spain; ^bInstitut Català d'Oncologia (ICO), Oncobell Program, IDIBELL. L'Hospitalet De Llobregat, Barcelona, Spain; ^cServicio de Oncología Médica, Hospital Universitario A Coruña, A Coruña, A Coruña, Spain; ^dServicio de Oncología Médica, Hospital General Dr. Balmis de Alicante, ISABIAL, Alicante, Spain; ^eFlow Cytometry Core Facility, Instituto de Investigación Sanitaria Puerta de Hierro-Segovia de Arana (IDIPHISA), Madrid, Spain; ^fServicio de Oncología Médica, Hospital Universitario Fundación Jiménez Díaz, Madrid, Spain; ^gFundación INCLIVA, Servicio de Oncología Médica, Hospital Clínico Universitario de Valencia, Valencia, Spain; ^hServicio de Oncología Médica, Hospital Universitario La Paz, Madrid, Spain; ⁱServicio de Oncología Médica, Hospital Alvaro Cunqueiro, Complejo Hospitalario Universitario de Vigo, Spain; ^jServicio de Oncología Médica, Hospital de la Santa Creu i Sant Pau, Barcelona, Spain; ^kVall Hebron Institute of Oncology (VHIO), Servicio de Oncología Médica, Hospital Universitari Vall d'Hebrón, Barcelona, Spain; ^lUnidad de Microscopía Óptica Avanzada, Instituto de Salud Carlos III, Majadahonda, Spain

ABSTRACT

Perioperative chemoimmunotherapy has significantly improved survival rates for non-small cell lung cancer (NSCLC). However, current tissue biomarkers remain inadequate, underscoring the need for more sensitive and accessible alternatives to monitor relapse risk. Intratumoral B-cells are increasingly recognized for their role in enhancing immunotherapy outcomes, yet the contribution of peripheral B-cells to immune surveillance remains unexplored. Peripheral B-cell immunophenotypes were analyzed from blood samples (at diagnosis, post-neoadjuvant, and at 6- and 12-months of adjuvant treatment) in 41 stage IIIA NSCLC patients treated with perioperative nivolumab plus chemotherapy, included in the NADIM clinical trial (NCT03081689). Results were correlated with 5-year survival outcomes and validated through unsupervised clustering. An increase in the percentage of total B-cells (CD19⁺CD20⁺) and naïve B-cells (CD19⁺CD20⁺CD24⁺CD38⁺CD27[−]CD10[−]), along with a reduction in CD20 expression on total B-cells, a decrease in the proportion of memory B-cells (CD19⁺CD20⁺CD24⁺CD38^{−/low}CD27⁺) and transitional B-cells (CD19⁺CD20⁺CD24⁺⁺CD38⁺⁺CD10⁺), was observed during the time encompassed between the end of neoadjuvant treatment and the posterior 6 months of adjuvant treatment. Higher levels of CD20 expression on total B-cells, along with an increased percentage of memory B-cells, or activated B-cells (CD19⁺CD20⁺CD25⁺), at 6- and 12-months of adjuvant treatment, were associated with increased survival. Conversely, higher levels of a newly described circulating population of CD19⁺CD20^{low}CD25^{low}CD27^{low} B-cells during adjuvant treatment were linked to disease progression. Perioperative nivolumab plus chemotherapy in resectable NSCLC patients induces significant changes in peripheral B-cells. The persistence of circulating memory B-cells during adjuvant treatment might play a crucial role in survival.

ARTICLE HISTORY

Received 29 November 2024
Revised 19 March 2025
Accepted 26 May 2025



KEYWORDS


B lymphocytes;
chemoimmunotherapy; flow
cytometry; NSCLC;
perioperative

Introduction

Lung cancer remains the leading cause of cancer-related mortality worldwide,¹ with non-small-cell lung cancer (NSCLC) comprising approximately 85% of all cases. Perioperative chemoimmunotherapy (ChIO) has revolutionized treatment, leading to enhanced overall survival (OS) rates and the establishment of a new standard of care.^{2–5} Five-year survival analysis from the NADIM clinical trial showed progression-free survival (PFS) and OS rates of 65.0% (95% CI 49.4–76.9) and 69.3% (95% CI 53.7–80.6), respectively, supporting the long-term benefit of perioperative nivolumab + chemotherapy.⁶

Clinically conventional biomarkers, such as Programmed Death-ligand 1 (PD-L1) and tumor mutational burden (TMB), have shown limitations on accurately identifying long-term survival after either perioperative ChIO⁶ or neoadjuvant immunotherapy (IO) monotherapy treatment.⁷ Additionally, these static biomarkers, determined at diagnosis, do not allow for the long-term anti-tumor immune response monitoring, thereby contributing to their lack of sensitivity in predicting long-term relapses. This limitation underscores the need for more specific and sensitive biomarkers that can evolve throughout the long follow-up periods that these patients experience in the new perioperative setting. On a similar note, the immune response

CONTACT Alberto Cruz-Bermúdez  alberto.cruz.bermudez@gmail.com  Medical Oncology Department, Puerta de Hierro Hospital, Manuel de Falla Street #1, Majadahonda, Madrid 28222, Spain

 Supplemental data for this article can be accessed online at <https://doi.org/10.1080/2162402X.2025.2513109>

© 2025 The Author(s). Published with license by Taylor & Francis Group, LLC.

This is an Open Access article distributed under the terms of the Creative Commons Attribution-NonCommercial License (<http://creativecommons.org/licenses/by-nc/4.0/>), which permits unrestricted non-commercial use, distribution, and reproduction in any medium, provided the original work is properly cited. The terms on which this article has been published allow the posting of the Accepted Manuscript in a repository by the author(s) or with their consent.

at the peripheral level has been associated with pathological responses⁸ or treatment related adverse events⁹ after perioperative immunotherapy, but no data exists regarding their potential impact on long-term survival.

Research on the adaptive immune system has predominantly focused on elucidating T cell mechanisms in the anti-tumor response. However, recent studies have increasingly highlighted the emerging role of B-cells through different mechanisms,¹⁰ specifically in the context of intratumoral tertiary lymphoid structures (TLSs),¹¹ whose abundance and degree of maturation have been associated with better outcomes in multiple types of solid tumors, including NSCLC.^{12–15} Yet, the role of peripheral B-cells in the context of neoadjuvant and adjuvant immunotherapies remains poorly understood. During neoadjuvant treatment, B-cells have been acknowledged as partakers in primary tumor responses.^{16,17} It is during adjuvant therapy when, their role in maintaining peripheral immunosurveillance could be critical for preventing disease recurrence. Emerging evidence suggests that the peripheral B-cell immunophenotype, particularly memory B-cells, may serve as a prognostic biomarker for treatment response and overall survival.^{18–20} Additionally, the noninvasive nature of blood sampling compared to tumor tissue biopsy offers a practical and readily accessible method for patient monitoring throughout treatment.

The aim of this study is to determine variations in the peripheral B immunophenotype throughout perioperative nivolumab plus chemotherapy treatment in resectable NSCLC patients and to evaluate its potential predictive value for pathological responses and survival.

Material and methods

Study population and design

Forty-six patients from 18 hospitals in Spain diagnosed with potentially resectable stage IIIA (TNM 7th edition) NSCLC were included in the open-label, multicenter, single-arm phase II NADIM clinical trial (NCT03081689). Patients were treated with neoadjuvant nivolumab (360 mg), combined with paclitaxel (200 mg/m²) and carboplatin (AUC 6, 6 mg/mL per min), on day 1 of each 21 day-cycle, for three cycles before surgical resection, followed by adjuvant nivolumab 240 mg Q2W for 4 months, and 480 mg Q4W for 8 months.²

Informed consent for the collection of research samples and study protocol were approved by the clinical research ethics committee of Hospital Puerta de Hierro and the Spanish Lung Cancer Group (SLCG) Board, in accordance with the International Conference on Harmonization Guidelines on Good Clinical Practice and the Declaration of Helsinki. Forty-one patients had available samples for B-cell analysis, and eight healthy individuals matched for age, sex, and smoking status made up the untreated control cohort. Control cohort samples and data were provided by IDIPHISA Biobank (ISCIII PT23/00015), with the appropriate approval of the Ethics and Scientific Committees.

Pathological response was evaluated after neoadjuvant nivolumab plus chemotherapy in surgical tissue samples (resected

primary tumor and lymph nodes) by blinded independent pathology review. Tumors were classified either as complete pathological response (CPR, 0% of viable tumor cells) or non-complete pathological response (NCPR, >0% of viable tumor cells). Patients who did not undergo surgery were excluded from the pathological response analysis.

Cohort was classified as patients with disease progression (DP) or patients without disease progression (NDP) according to their status at 60 months of follow-up (this being the end of an established follow-up by trial protocol). Progression-free survival (PFS) was set as the time from diagnosis to objective tumor progression or cancer-related death. Similarly, overall survival (OS) was defined as the time from diagnosis to date of cancer-related death. COVID-19 and other causes of death not related to disease progression were considered as loss of follow-up at the time of death.⁶

Peripheral blood mononuclear cells (PBMCs) isolation

Peripheral blood samples were obtained at pre-treatment, post-neoadjuvant treatment (before surgery), and at 6 and 12 months of adjuvant treatment. Peripheral blood was collected in EDTA tubes and processed within 24 h of extraction. Samples were diluted to 1:1 in RPMI 1640, and peripheral blood mononuclear cells (PBMCs) were extracted by density gradient with Lymphoprep (Stemcell). PBMCs were cryopreserved in 1:1 RPMI/FBS +10% DMSO freezing medium until use.

Flow cytometry

About 5 to 8 million cells per sample were thawed and stained with fluorochrome conjugated antibodies (Table S1) to define lymphocyte subpopulations of B-cells. Cells were incubated with antibodies for 30 min at 4°C in FACS buffer (PBS +5% FBS), and DAPI staining (to exclude dead cells) prior to acquisition in a MACSQuant10 flow cytometer with MACSQuantify 2.8 software (Miltenyi Biotec).

Immunophenotype analysis

Samples were analyzed using the FlowJo LLC v10 software (RRID: SCR_008520). Traditional supervised gating strategy was performed setting the positivity threshold of fluorescence minus one (FMO) controls (gating strategy and FMO are shown in Figure S1A–B). Total B-cells (CD19⁺CD20⁺) were classified as naïve B-cells (CD19⁺CD20⁺CD24⁺CD38⁺CD27[−]CD10[−]), memory B-cells (CD19⁺CD20⁺CD24⁺CD38^{−/low}CD27⁺) or transitional B-cells (CD19⁺CD20⁺CD24⁺⁺CD38⁺⁺CD10⁺). In addition, the percentage of CD25⁺ activated B-cells was calculated for the total B-cells (CD19⁺CD20⁺CD25⁺) and within each subpopulation. We studied circulating B-cell subtypes in terms of population proportions of total B-cells and marker expression in each subpopulation, measured with median fluorescence intensity (MFI). A median of 234,116 events (IQR: 153,110–339,929) was obtained across a total of 113 samples. Only populations comprising at least 100 cells at sample level were considered for further analysis.

An unsupervised analysis was performed in FlowJo, where 20,000 CD19⁺CD20⁺ cells (evenly distributed between DP and

NDP patients) were concatenated into a single.fcs file. The FlowSOM algorithm²¹ (RRID:SCR_01689) generated 10 clusters, later visualized as t-SNE and heatmaps in ClusterExplorer. Automated cluster assignment across all samples and events was performed using HyperFinder. Further details are available in the supplementary material.

CD20^{low}CD25^{low}CD27^{low} prognosis signature for long-term survival was determined by stepwise selection of each of the three markers (Figure S1C). The threshold for each marker was set as the median of the respective population MFI (CD19⁺CD20⁺ general B-cells for CD20 MFI, CD19⁺CD20⁺CD25⁺ activated B-cells for CD25 MFI, and CD19⁺CD20⁺CD24⁺CD38^{-/low}CD27⁺ memory B-cells for CD27 MFI).

Immunofluorescences of tertiary lymphoid structures

Multiplexed immunofluorescences with anti-CD3, CD20, CD23, and DAPI were performed on FFPE surgical specimens from 18 patients to quantify tertiary lymphoid structures (TLS). Whole slide images were acquired using a Stellaris 8 confocal microscope (Leica) at 10X magnification. TLSs were determined as aggregates of mixed T and B-cells of more than 20 cells. Subsequently, mature TLSs were defined as those with CD23⁺ stain. TLSs were evaluated and counted twice by two independent reviewers, who were blinded to clinical information and each other's results. For further details, please refer to the supplementary material.

Statistics

Given the low sample size, we presumed a non-normal distribution. Wilcoxon rank test was used to compare paired samples from the same patient at different timepoints. Mann–Whitney U test was performed to compare between independent groups of patients. Bivariate correlations using Spearman's rho were established between the flow cytometry populations and the density of TLSs. Two-tailed *p* values <0.05 were considered statistically significant.

Parameters showing areas under the curve (AUC)>0.70 with significant *p*-value in receiver operating characteristic (ROC) analysis were considered as relevant biomarkers. Kaplan–Meier survival analysis with log-rank test was performed between groups of patients categorized by the value with highest specificity/sensitivity ratio determined by ROC analysis between DP and NDP patients.

Statistical analyses were performed using R 4.3.2 and confirmed with GraphPad Prism v.8 (RRID:SCR_002798).

Data availability

The data generated in this study are available upon request from the corresponding author.

Results

Cohort and sample characteristics

The study cohort is composed of 41 out of 46 patients included in the NADIM clinical trial (89.1%, of the complete trial

cohort) who had available PBMCs. Median follow-up was 60.0 months (IQR 60.0–60.0). Five-year clinical outcomes of the complete cohort have been published elsewhere.⁶

Baseline characteristics of the 41 patients in this study are summarized in Table 1.^{2,6} Ten patients experienced lung cancer disease progression, and eight patients died because of their lung cancer disease.

Peripheral B lymphocyte immunophenotype was characterized in all available blood samples (Table S2), specifically at pre-treatment (*n* = 29), post-neoadjuvant treatment but pre-surgery (*n* = 29), at 6 months of adjuvant treatment (*n* = 27) and at 12 months of adjuvant treatment (*n* = 28).

Changes in peripheral B-cell immunophenotype through perioperative ChIO

First of all, we explored changes in circulating B immunophenotype between different blood samples through the complete perioperative treatment (Figure 1, Figure S2). Immunophenotypic analysis of PBMCs revealed an increase in total B-cells (CD19⁺CD20⁺) between post-neoadjuvant treatment and 12 months of adjuvant treatment (*p* = 0.027, Figure 1a, Figure S2a), specifically, this increase is observed earlier at 6 months of adjuvant treatment (*p* = 0.026, Figure 1a, Figure S2a). Moreover, a decrease in CD20 expression in total B-cells was identified in the same period (*p* = 0.024, Figure 1b, Figure S2b). No changes were identified in CD25⁺ activated B-cells (CD19⁺CD20⁺CD25⁺, Figure 1c, Figure S2c).

Referring to B-cell subtypes, an increase in the percentage of naïve B-cells (CD19⁺CD20⁺CD24⁺CD38⁺CD27⁺CD10⁺) was identified between post-neoadjuvant and 12 months of adjuvant treatment (*p* = 0.001, Figure 1d, Figure S2d). Similar to previous results, this increase occurred during the first 6 months of adjuvant treatment (*p* = 0.005, Figure 1d, Figure S2d). On the contrary, during the same period, there was a drop in transitional B-cells (CD19⁺CD20⁺CD24⁺CD38⁺CD10⁺; *p* = 0.021, Figure 1e, Figure S2e) and memory B-cells

Table 1. Cohort clinical and demographic characteristics.

Characteristic	Values
Median age, years (IQR)	62 (57.5–70)
Sex, n (%)	
Male	29 (70.7)
Female	12 (29.3)
Histology, n (%)	
Adenocarcinoma	25 (61.0)
Squamous carcinoma	12 (29.3)
NOS/Undifferentiated	4 (9.8)
PD-L1, n (%)	
≥50%	13 (31.7)
1%–49%	3 (7.3)
<1%	8 (19.5)
Undetermined	17 (41.5)
Pathological response, n (%)	
Complete (CPR)	26 (63.4)
Non-Complete (NCPR)	13 (31.7)
Not operated	2 (4.9)
5-year Progression Free Survival, median (95%CI)	75.30 (58.92–85.89)
5-year Overall-survival, median (95%CI)	79.50 (63.06–89.21)
Median Follow-up, months (IQR)	60 (60.0–60.0)

IQR interquartile range, NOS not-other specified, CI confidence interval.

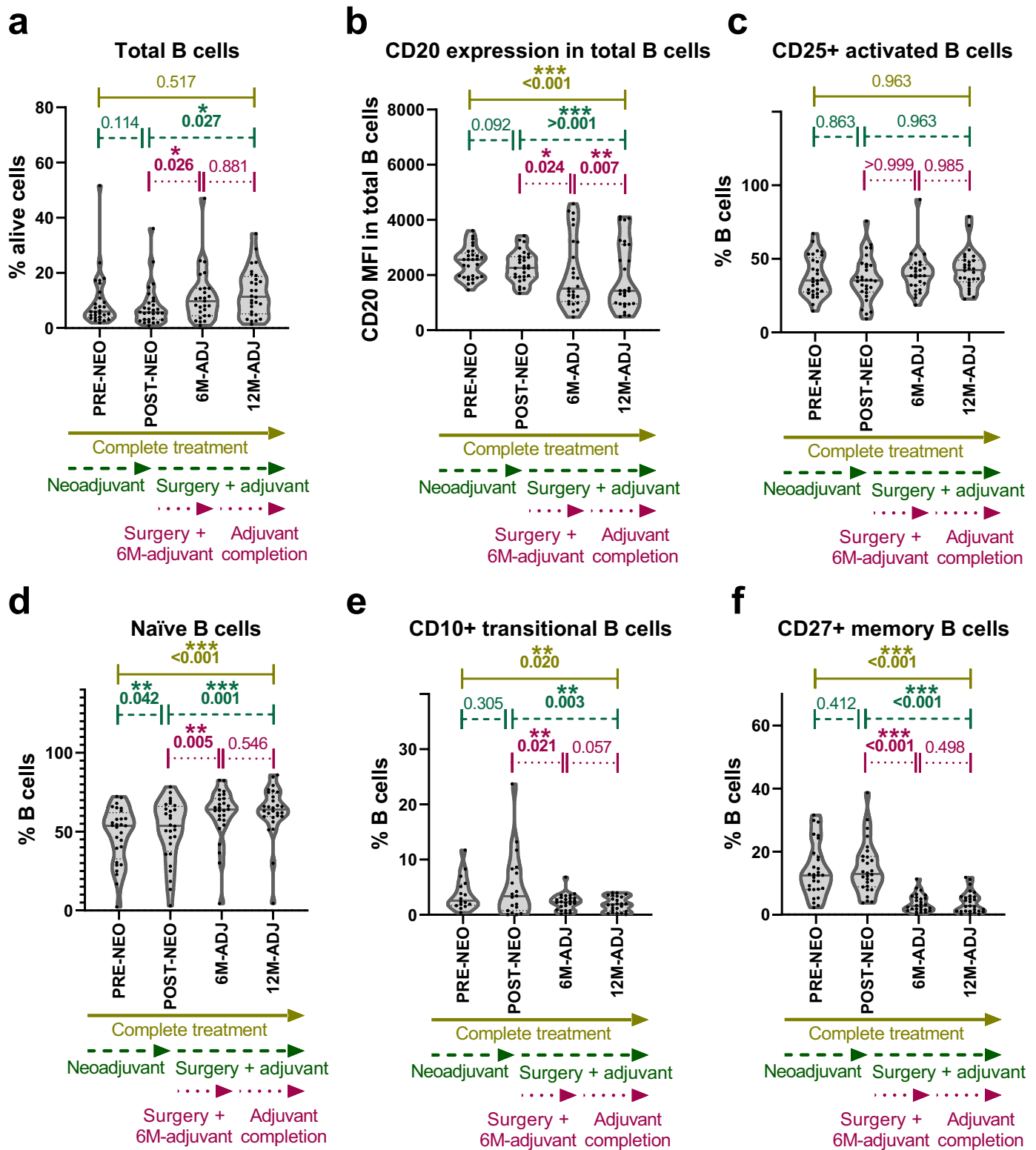


Figure 1. Changes in circulating B-cell phenotype throughout treatment. (a) %CD19⁺CD20⁺ total B-cells. (b) CD20 MFI in total B-cells. (c) %CD25⁺ activated B-cells (CD19⁺CD20⁺CD25⁺). (d) %CD19⁺CD20⁺CD24⁺CD38⁺CD27[−]CD10[−] naïve B-cells. (e) %CD19⁺CD20⁺CD24⁺CD38⁺CD10⁺CD27[−] transitional B-cells. (f) %CD19⁺CD20⁺CD24⁺CD38⁺CD27⁺ memory B-cells. All samples are represented, p-values correspond to Wilcoxon test comparisons only for paired samples. NEO neoadjuvant, PRE pre-treatment, POST post-neoadjuvant treatment, ADJ adjuvant treatment, MFI median fluorescence intensity.

(CD19⁺CD20⁺CD24⁺CD38^{−/low}CD27⁺; $p < 0.001$, Figure 1f, Figure S2f). Our results show multiple changes in peripheral B-cells during perioperative nivolumab + chemotherapy treatment in NSCLC patients. We describe an increase in the

proportion of total B-cells and naïve B-cells among PBMCs during surgery and adjuvant treatment start, along with a drop in CD20 expression and percentage of transitional and memory B-cells.

High levels of CD20 expression, memory, or activated B-cells in peripheral blood during adjuvant treatment are associated with long-term survival independently of intratumoral TLSs

First, we explored differences in circulating B immunophenotype between patients and controls. A higher proportion of total B-cells, a higher expression of CD20, a decreased proportion of naïve B-cells, and a trend toward a higher proportion of memory B-cells were observed in controls compared to patients (Figure S3).

Secondly, we tested for differences regarding pathological response status (CPR vs NCPR, Figure S4) and histology (adenocarcinoma vs squamous, Figure S5). No differences in the main B-cell populations nor marker expression in any of the extractions were observed for these comparisons.

We further aimed to determine potential differences by classifying patients based on whether they experienced disease progression (Figure 2, table S3). At pre-treatment and post-neoadjuvant treatment, no differences between patients with disease progression (DP) and without disease progression (NDP) were observed. However, in patients with long-term DP, lower expression of CD20 in total B-cells was detected at 6 months ($p = 0.017$) and 12 months ($p = 0.003$) of adjuvant treatment (Figure 2b). Moreover, a reduced proportion of CD25⁺ activated B-cells was also identified in DP compared to NDP at 6 months of adjuvant treatment ($p = 0.009$) (Figure 2c). Finally, DP patients presented a lower percentage of CD27⁺ memory B-cells compared to NDP patients at 6 months ($p = 0.001$) and 12 months of adjuvant treatment ($p = 0.015$) (Figure 2f).

ROC curves for DP and Kaplan–Meier survival analyses of CD20 expression, CD25⁺, and CD27⁺ memory B-cell populations were carried out in samples during adjuvant treatment (Figure 3) and before adjuvant treatment (Figure S6).

We confirmed as valuable biomarkers of long-term DP during adjuvant treatment the expression of CD20, and percentages of CD25⁺ activated and CD27⁺ memory B-cells at 6 and 12 months of adjuvant treatment, all with AUC values above 0.7 (Figure 3a). Next, Kaplan–Meier survival analyses were conducted. Patients with higher values of CD20 expression or higher percentages of CD25⁺ activated and CD27⁺ memory B-cells, determined by ROC curves at 6 and 12 months of adjuvant treatment, showed statistically significant longer PFS and OS compared to patients with lower values (Figure 3b). A similar trend is observed when classifying patients by median and tertiles (figures. S7–8).

Although these B-cell subpopulations did not show prognostic capacity at pre-treatment and post-neoadjuvant treatment by ROC curve analysis, some of them presented a trend toward longer PFS and OS for those patients with higher values (Figure S6).

We further wanted to know if changes in peripheral B immunophenotype were associated with disease progression (table S4). Changes throughout treatment were then evaluated, stratifying the patients according to whether or not they had disease progression. We compared the relative change (fold change) between paired samples at two sequential timepoints. CD20 expression and proportion of CD25⁺ activated and

CD27⁺ memory B-cells were significantly more reduced in patients with DP compared to patients with NDP (Figure S9).

Finally, to investigate whether the peripheral B-cell immunophenotype was associated with the intratumoral immune microenvironment after neoadjuvant treatment, we analyzed the correlations between B-cell subpopulations in peripheral blood and the density of total TLSs and mature TLSs in resected tumor specimens (Figure S10). However, we did not observe any significant correlations at pre-treatment, post-neoadjuvant, nor at 6 and 12 months of adjuvant treatment with the density of total or mature TLSs (table S5).

Briefly, higher levels of CD20 expression in total B-cells, plus higher proportions of CD25⁺ activated and CD27⁺ memory B-cells in circulating immunophenotype during adjuvant treatment, are predictors of longer survival in our cohort. In addition, a heavier reduction of these populations is prognostic for long-term disease progression. Moreover, peripheral B immunophenotype is not associated with intratumoral density of total or mature TLSs.

Unsupervised analysis confirms differences between circulating B-cells according to disease progression

In order to confirm the identified differences found in circulating B-cells between DP and NDP, we next performed unsupervised clustering analysis with the FlowSOM algorithm²¹ in a representative downsampled subcohort. Graphs are built upon cell phenotype similarity. As such, groups of cells that share similar phenotypes are identified as a node, and node size is proportional to the number of cells within that population.

B-cells from 6 to 12 months of adjuvant treatment blood samples were reduced and concatenated and subsequently grouped in 10 different clusters (Figure S11A). Visualization of these B-cell subpopulations with *t*-distributed stochastic neighbor embedding (*t*-SNE) confirmed the resemblance within these 10 clusters generated by FlowSOM (Figure S11B). Relative expression levels of markers for each cluster are represented in a heatmap (Figure S11C), where each column reflects the relative intensity of each of the seven markers, whilst each row corresponds to each of the 10 clusters computed by FlowSOM.

Differences between cells provided by DP and NDP patients were observed in clusters 0, 7, and 9 in 6 months adjuvant treatment samples, and also in clusters 0, 6, and 7 in 12 months adjuvant treatment samples (Figure 4a).

To confirm these differences, HyperFinder algorithm was applied in order to establish a gating strategy applicable to unreduced samples. At 6 months of adjuvant treatment, clusters 7 and 9 showed significantly higher percentages of cells in NDP compared to DP (C7: $p = 0.018$; C9: $p = 0.002$). In contrast, also at 6 months of adjuvant treatment, there was a trend toward to higher proportions of cells in DP compared to NDP in cluster 0 ($p = 0.080$). Adjuvant treatment samples at 12 months display a higher percentage of cells in DP compared to NDP in cluster 0 ($p = 0.007$); as opposed to cluster 6, in which most of the cells are provided by NDP ($p = 0.008$). A trend is also observed in cluster 7, with a higher number of cells belonging to NDP ($p = 0.081$) (Figure 4b).

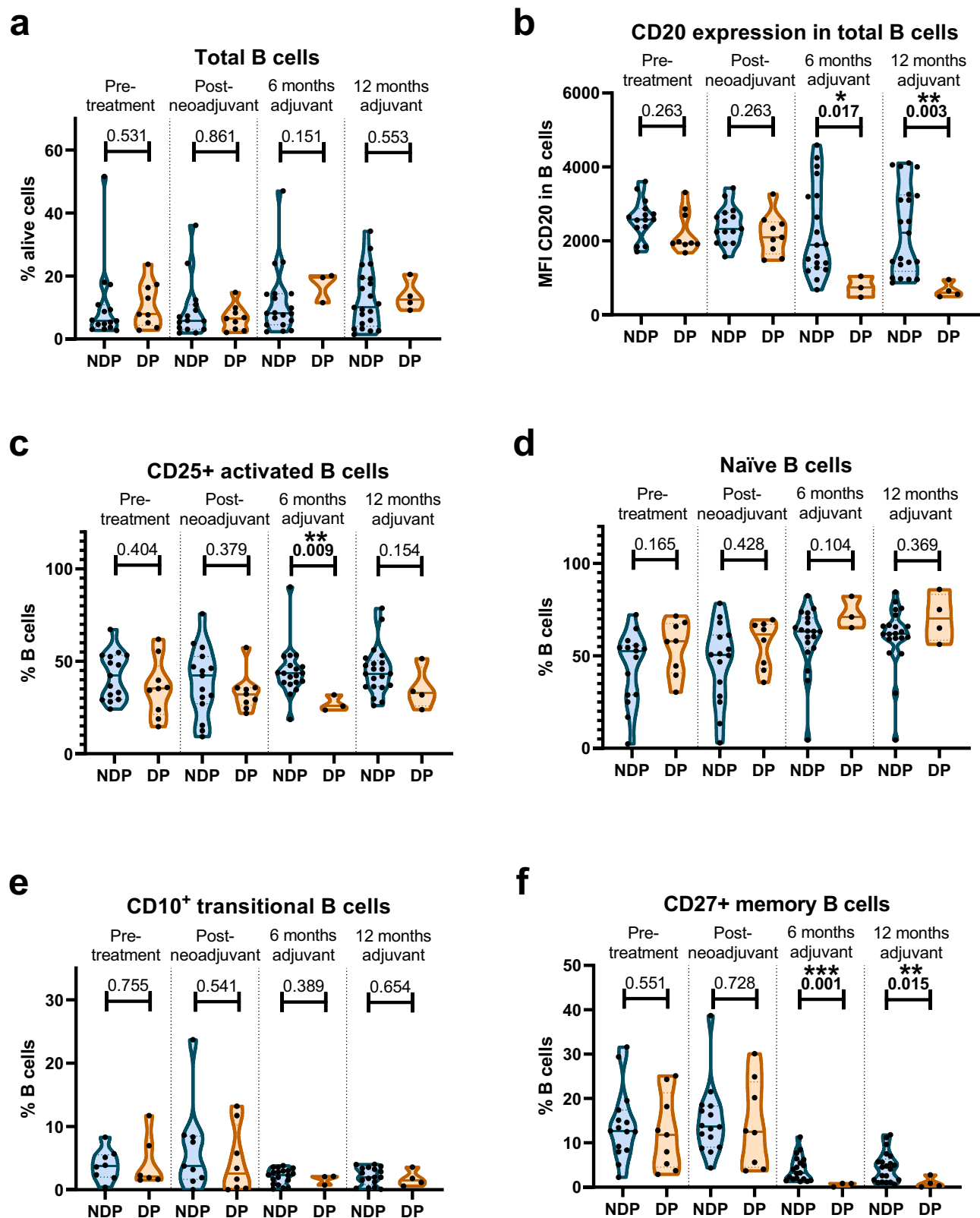


Figure 2. Differences in circulating B phenotype classifying patients according to disease progression status. (a) %CD19⁺CD20⁺ total B-cells. (b) CD20 MFI in total B-cells. (c) %CD19⁺CD20⁺CD25⁺ activated B-cells. (d) %CD19⁺CD20⁺CD24⁺CD38⁺CD27⁻CD10⁻ naïve B-cells. (e) %CD19⁺CD20⁺CD24⁺CD38⁺CD27⁻CD10⁺ transitional B-cells. (f) %CD19⁺CD20⁺CD24⁺CD38⁻CD27⁺ memory B-cells. Non-parametric U-Mann Whitney test, p-values under 0.05 were considered statistically significant. Pre: pre-treatment, post: post-neoadjuvant treatment, DP: disease progression, NDP: non-disease progression, MFI: median fluorescence intensity.

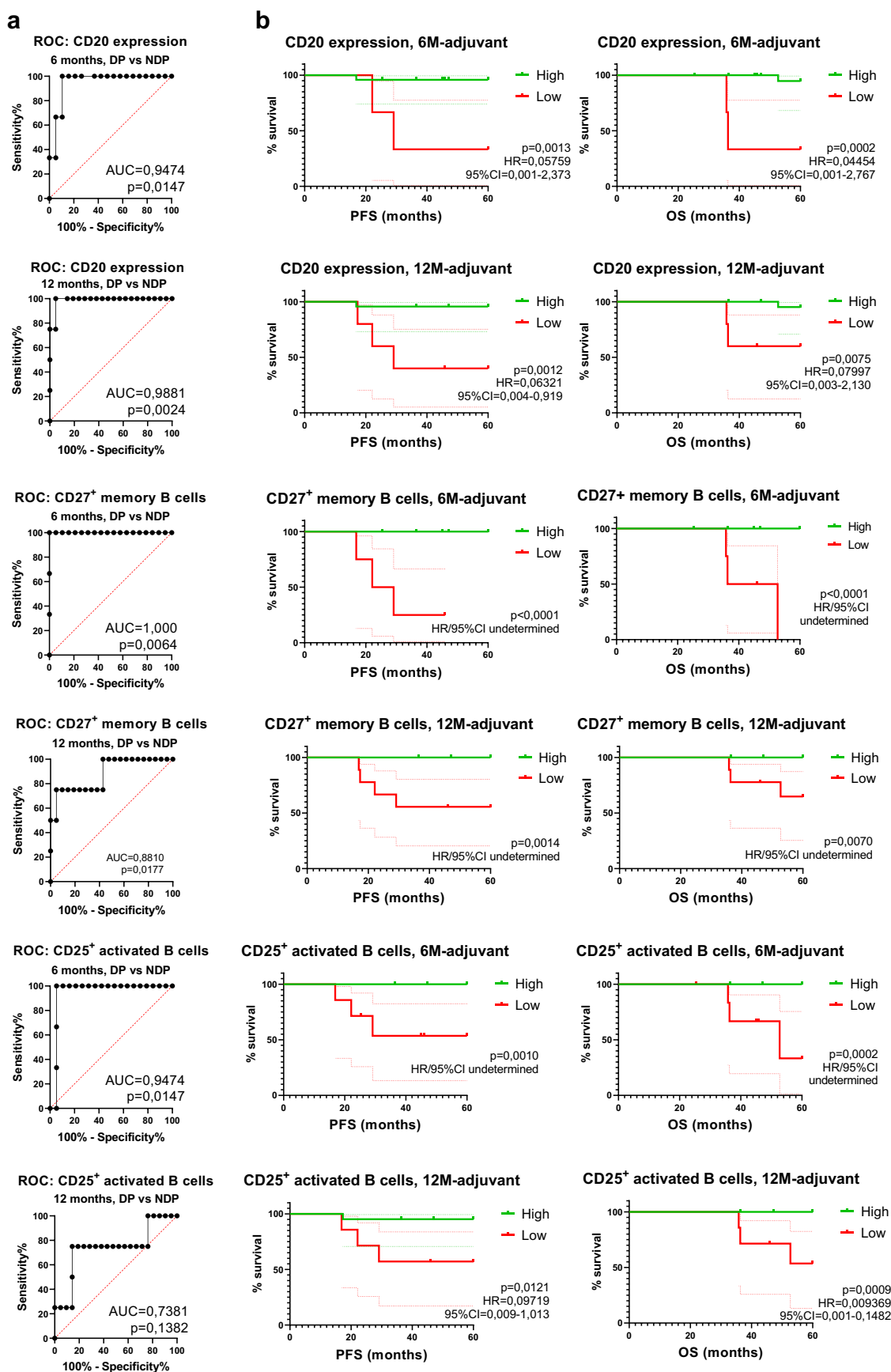


Figure 3. Predictive ability of progression and survival of CD20 expression, %CD27⁺ memory and %CD25⁺ activated B-cells at 6/12 months of adjuvant treatment. a) ROC curve analysis. b) Kaplan Meier analysis of PFS and OS with log-rank test for CD20 expression at 6 ($n = 24 \geq 844$, $n = 3 < 844$) and 12 ($n = 23 \geq 954$; $n = 5 < 954$) months; %CD27⁺ memory B-cells at 6 ($n = 23 \geq 1.3\%$, $n = 4 < 1.3\%$) and 12 ($n = 19 \geq 0.97\%$, $n = 9 < 0.97\%$) months; and %CD25⁺ activated B-cells at 6 ($n = 20 \geq 32\%$, $n = 7 < 32\%$) and 12 ($n = 21 \geq 34.8\%$, $n = 7 < 34.8\%$) months of adjuvant treatment. P-values less than 0.05 were considered statistically significant. ROC: receiver operating characteristic; AUC: area under the curve; DP: disease progression; NDP: non-disease progression; PFS: progression-free survival; OS: overall survival; HR: hazard ratio; CI: confidence interval.

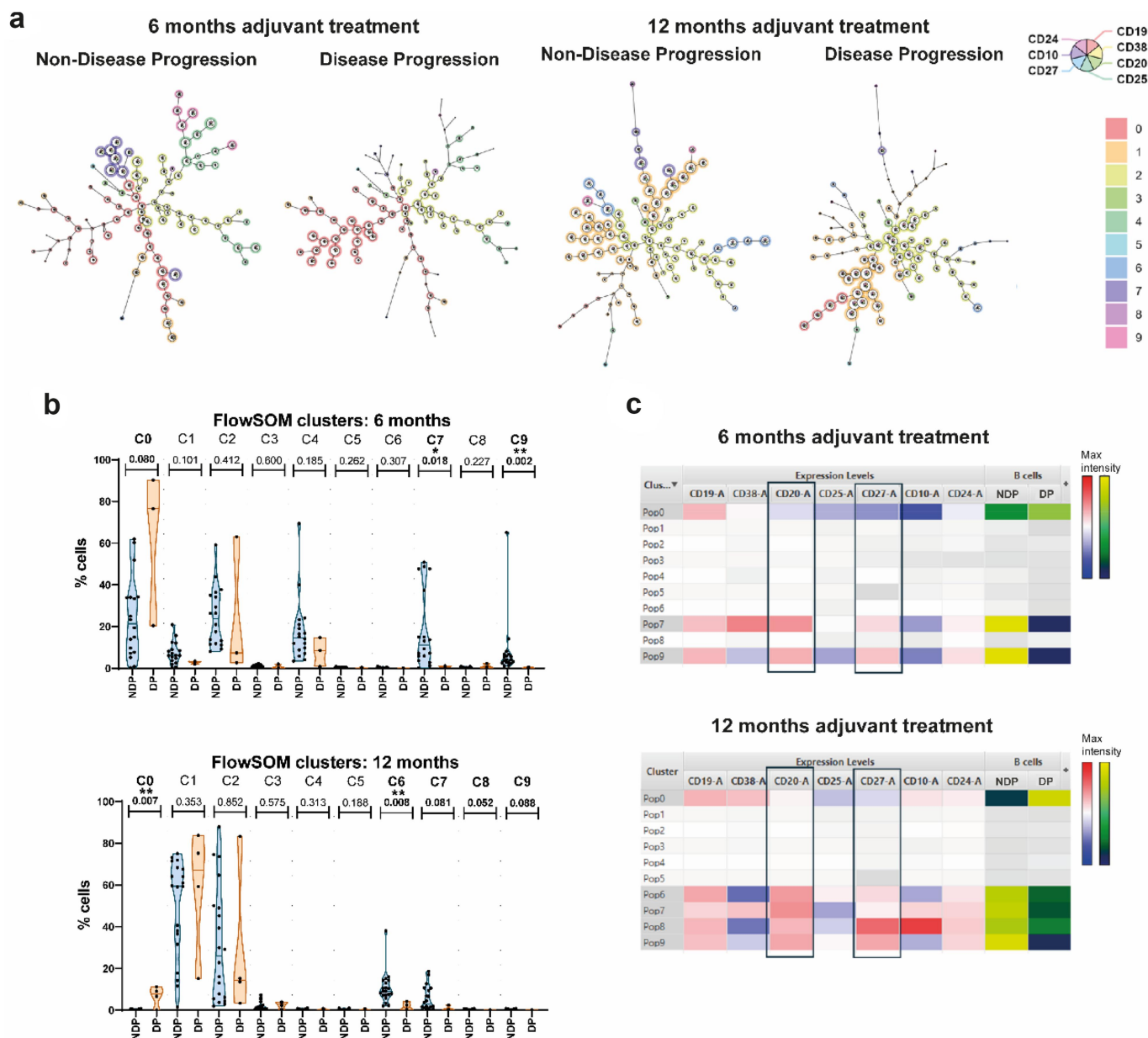


Figure 4. Differences between NDP and DP in circulating B phenotype at 6/12 months of adjuvant treatment determined by computerized unsupervised analysis (FlowSOM). a) Minimal spanning tree representation of cells from DP and NDP at 6 and 12 months of adjuvant treatment. Clusters generated independently for each representation, phenotypes corresponding to cluster numbering are not matched between 6- and 12-month samples. b) Statistical analysis of the percentage of cells contributed to each cluster based on disease progression. Each point represents the percentage of cells a patient contributes to the examined cluster relative to the patient's total B-cells (6 months: NDP $n = 18$, DP $n = 3$; 12 months: NDP $n = 20$, DP $n = 4$). U-Mann Whitney test, p-values less than 0.05 were considered statistically significant. c) Relative expression of markers in clusters with significant differences at 6 and 12 months of adjuvant treatment. Red-blue scale, relative expression of B-cell panel markers for clusters with significant differences; yellow-green scale, relative enrichment of B-cells contributed by patients with or without disease progression.

With the objective of characterizing relevant markers for each cluster, we compared expression levels of the seven markers that compose the panel (Figure 4c). Both at 6 and 12 months of adjuvant treatment, cluster 0 is enriched with cells belonging DP and it shows lower relative levels of CD20 and CD27 markers. Conversely, in clusters 7 and 9 at 6 months-adjuvant and clusters 6 to 9 at 12 months-adjuvant treatment, which are enriched with cells from NDP, a higher expression of CD20 and CD27 is detected.

In conclusion, unsupervised clustering analysis of circulating B phenotype confirms that a higher expression of CD20

and CD27 markers through adjuvant treatment is prognostic of long-term survival.

Higher levels of circulating $CD19^+CD20^{low}CD25^{low}CD27^{low}$ population during adjuvant treatment are associated to disease progression

The relationship between disease progression and the relative lower expression of CD20 and decreased percentages of $CD25^+$ activated and $CD27^+$ memory B-cells, led to the proposal of a population of interest characterized by the low expression of

these markers (CD19⁺CD20^{low}CD25^{low}CD27^{low}, Figure S1C). This population consists of a mixture of naïve, transitional, memory, and other undefined B-cell subpopulations (Figure 5a).

Throughout the complete treatment, we identified an increase in this population between post-neoadjuvant treatment and 6 months of adjuvant treatment ($p = 0.003$, Figure S12A).

Regarding its prognostic value, during neoadjuvant treatment, there were no differences between DP and NDP, nor are there any disparities at pre-treatment or post-neoadjuvant treatment (pre-treatment: $p = 0.347$, post-neoadjuvant: $p = 0.215$, Figure S12B). Exploring this population during adjuvant treatment, at 6 months of adjuvant treatment, DP patients showed a higher percentage of CD19⁺CD20^{low}CD25^{low}CD27^{low} B-cells compared to NDP patients ($p = 0.005$, Figure 5b). Same trend can be observed at 12 months of adjuvant treatment ($p = 0.083$, Figure 5b). This B-cell population turned out to be a strong prognostic marker of disease progression according to the ROC curve analysis only throughout adjuvant treatment (Figure 5c). We classified patients as high/low based on the cutoff point with the highest sensitivity/specificity ratio in the ROC curve. Although ROC curve analysis did not validate prognostic ability during neoadjuvant treatment (Figure S12C), there was a trend toward prolonged PFS for those patients with a lower percentage of CD19⁺CD20^{low}CD25^{low}CD27^{low} B-cells at pre-treatment ($p = 0.063$). This trend turned out to be significant at post-neoadjuvant treatment ($p = 0.044$) (Figure S12D). However, the greatest contrast in terms of survival was detected in adjuvant treatment at 6 and 12-months, when patients with a low percentage of CD19⁺CD20^{low}CD25^{low}CD27^{low} cells showed longer PFS and OS compared to patients with a high percentage of this population (Figure 5d).

Finally, we analyzed the CD19⁺CD20^{low}CD25^{low}CD27^{low} population in healthy controls (HC). This population was almost absent in HC compared to pre-treatment patient samples ($p < 0.001$, Figure 5e), demonstrating its potential diagnostic value in distinguishing between HC and patients, as shown by the ROC curve analysis (AUC = 0.9397, Figure 5f).

In summary, in our cohort of patients with locally advanced NSCLC undergoing perioperative treatment with nivolumab + chemotherapy; lower percentages of the circulating B-cell population CD19⁺CD20^{low}CD25^{low}CD27^{low} at post-neoadjuvant treatment, 6 and 12 months of adjuvant treatment are indicative of long-term survival.

Discussion

The objective of our study was to investigate the circulating B-cell phenotype in a cohort of stage IIIA potentially resectable NSCLC patients undergoing perioperative nivolumab plus chemotherapy. While no significant changes in B-cell phenotype were observed during the neoadjuvant treatment period, a generalized increase in the percentage of B lymphocytes and a decrease of CD20 expression were detected in the period between surgery and the first 6 months of adjuvant treatment. Furthermore, the analysis of B-cell subpopulations during this interval revealed an increase in the proportion of naïve B-cells, accompanied by a corresponding decrease in the percentages

of CD10⁺ transitional and CD27⁺ memory B-cells. When stratifying patients according to disease progression, flow cytometry analysis of 6- and 12-month adjuvant samples revealed that patients with disease progression (DP) following completion of treatment exhibited lower levels of CD20 expression, as well as reduced percentages of memory CD27⁺, and activated CD25⁺ B-cells, compared to patients without disease progression (NDP). This association was corroborated by unsupervised computerized analysis, which mitigated potential biases inherent to traditional analytical methods. Moreover, a prognostic signature, characterized by a low percentage of circulating CD19⁺CD20^{low}CD25^{low}CD27^{low} B lymphocytes, was developed and it successfully identified patients with longer PFS and OS.

The marked decrease in CD20 expression, as well as in the percentage of activated and memory B-cells observed between surgery and the first 6 months of adjuvant therapy, may be attributable to the resection of the tumor and draining lymph nodes. This presumably eliminated the primary source of tumor antigens and B-cell activation centers (including tumor-associated TLSs and germinal centers in draining lymph nodes) for antitumoral B-cell immunity in these patients with locally advanced disease. However, we did not observe any relationships between the density of TLSs in the resected tumors and peripheral populations, which would support a limited role of the tumor's B-cell component in influencing overall immune populations. Instead, the role of resected lymph nodes or the loss of tumor antigens may be more relevant.

In fact, preclinical models have demonstrated the negative impact of completely removing the tumor and lymph nodes on the antitumor immune response, although this can be mended through adjuvant therapy.^{22–24} This evidence further supports the perioperative immunotherapy approach versus the adjuvant-only approach. The perioperative strategy would promote the generation of a strong immune response in the presence of the tumor, while adjuvant therapy, after the tumor and draining lymph nodes are removed, would facilitate the maintenance of an immunological memory.

In this regard, we observed that patients who maintained minimal levels of memory B-cells during adjuvant therapy exhibited longer survival, in contrast to those who experienced disease progression, in which these levels were nearly undetectable in our setting. Similar findings have been reported in cancer patients treated with immunotherapy, where memory B-cells appear to be associated with better disease control and improved survival.^{18,24}

Memory B-cells play a crucial role in initiating an immediate response upon encountering their specific antigen.²⁵ The persistence of memory B-cells may reflect an immunosurveillance mechanism, in which the appearance of new microscopic metastases and associated tumor antigens could trigger a rapid and effective antitumor response. Similarly, the expression of CD25, which is associated with an activated phenotype, and CD20, which is essential for effective BCR signaling, could suggest increased CD19⁺CD20⁺ B-cell activity.^{20,25}

These findings reinforce the idea that surgery, beyond its role as a radical treatment for tumor elimination, could also function as a systemic immunomodulatory element.^{22–24} Moreover, surgery could be tailored in the future based on

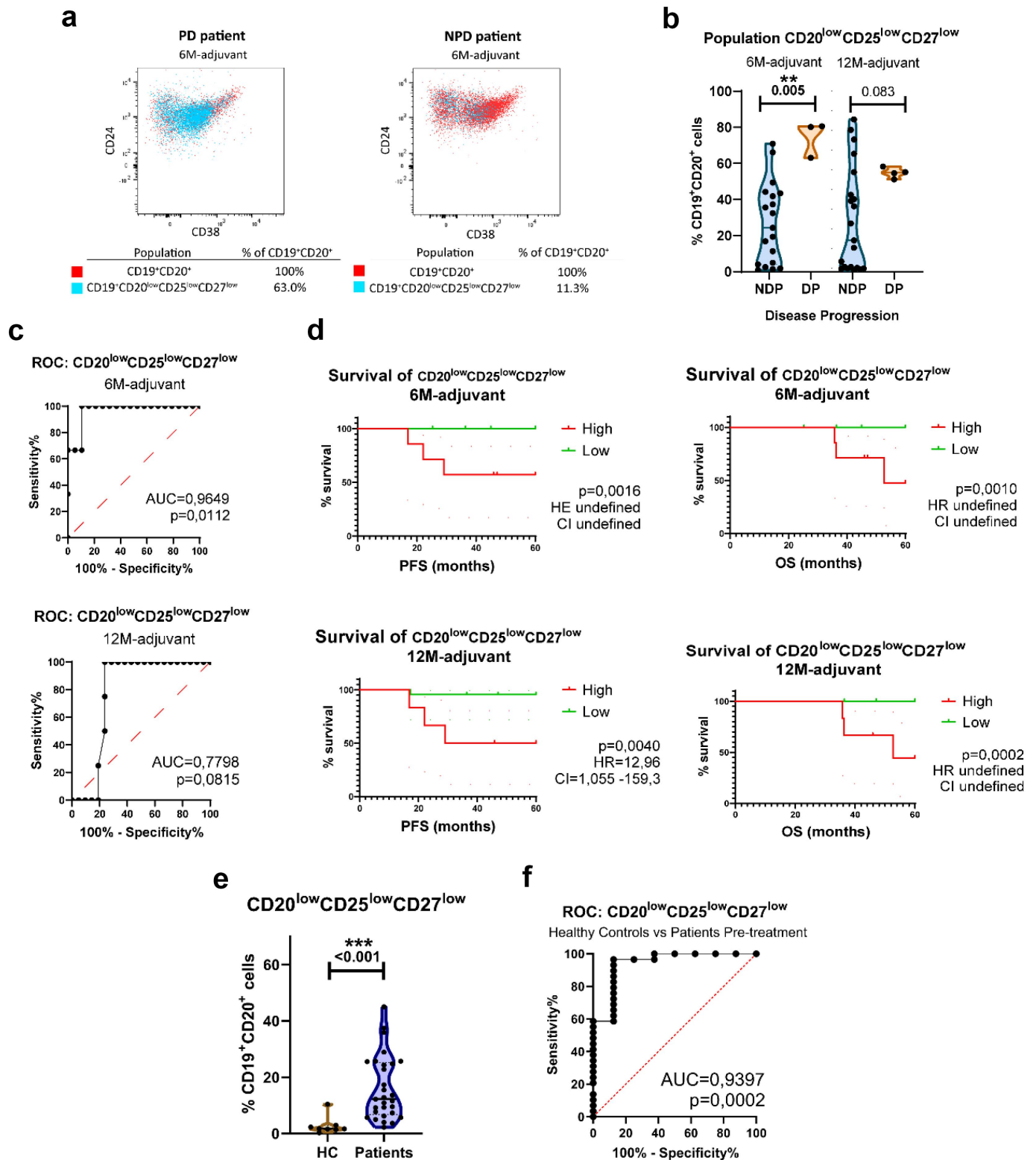


Figure 5. Prognostic signature of circulating CD19⁺CD20^{low}CD25^{low}CD27^{low} B-cells of long-term progression at 6/12 months of adjuvant treatment. a) examples of localization of CD19⁺CD20^{low}CD25^{low}CD27^{low} population (blue) over total B-cells (red) and percentages with respect to total B-cells, in representative samples from a DP patient and NPD patient at 6 months of adjuvant treatment. b) Differences in the percentage of cells of CD19⁺CD20^{low}CD25^{low}CD27^{low} population, according to disease progression. U-Mann Whitney test. c) ROC curve analysis between DP and NDP. d) Progression free survival (PFS) and overall survival (OS), classifying patients in high/low percentage according to the cutoff with the highest specificity/sensitivity ratio of the ROC curve. 6 months: $n = 7 \geq 58$, $n = 20 < 58$; 12 months: $n = 6 \geq 58$, $n = 22 < 58$. Log-rank test. e) Differences between healthy controls and patients at pre-treatment of CD19⁺CD20^{low}CD25^{low}CD27^{low} population. f) ROC curve analysis between HC and patients at pre-treatment. HC: healthy controls, ROC: receiver operating characteristic; AUC: area under the curve; HR: hazard ratio; CI: confidence interval.

patient characteristics and antitumor immune response; similar to the current goal of personalizing adjuvant therapy and adapting it to the individual needs of each patient.

Beyond this, our results support the possibility of monitoring patients after neoadjuvant therapy based on the maintenance of antitumor memory, potentially allowing for the future personalization of adjuvant treatment in terms of both its duration (e.g., reducing adjuvant treatment phase in patients with strong antitumor immune memory) and the pharmacological mechanisms to be targeted (e.g., activating pathways that promote the maintenance of antitumor memory if it is insufficient). B-cells, in particular, emerge as a relevant compartment in peripheral blood for this purpose, in which the described CD19⁺CD20^{low}CD25^{low}CD27^{low} B lymphocyte population could be useful to predict potential disease relapses after neoadjuvant treatment. Interestingly, this population is reduced in healthy individuals, reinforcing the role of cancer as a disease associated with systemic immune changes, as well as the negative impact of this population on peripheral immunity. In this regard, this population may not represent a group of cells with a specific, unique function, as it overlaps with classic naïve, transitional, and memory populations, but it could serve as a biomarker that indicates a generally more inhibited peripheral blood B-cell status.

We acknowledge that this study has some limitations. First, the limited number of patients recruited in the NADIM trial restricted our analysis to a small subset of cases. However, despite this constraint, NADIM represents the largest cohort in the NSCLC perioperative setting with a five-year follow-up to date. Furthermore, the immune populations identified by flow cytometry, as well as the definition of the CD19⁺CD20^{low}CD25^{low}CD27^{low} population, are based on median fluorescence intensity (MFI), which is highly dependent on technical settings and requires methodological adaptation for other laboratories. Nonetheless, these limitations do not invalidate the exploratory, hypothesis-generating nature of this study, which provides promising insights into the largely unexplored field of adjuvant immunotherapy monitoring and long-term survival after perioperative ChIO.

In conclusion, perioperative nivolumab plus chemotherapy induces significant changes in peripheral blood B-cells between surgery and the first 6 months of adjuvant treatment. The maintenance of circulating B-cell phenotype with increased memory, activation, and CD20 expression during adjuvant treatment is relevant for long-term survival and could be useful for monitoring the antitumor immune response, as well as personalizing adjuvant treatments following neoadjuvant nivolumab plus chemotherapy. Further research is required to validate these findings in larger cohorts.

Acknowledgments

We extend our gratitude to the patients and their families, the clinical teams involved, and the entire Spanish Lung Cancer Group, as well as BMS, for their invaluable contributions to making this study possible. The authors wish to thank the IDIPHISA Biobank (ISCIII Platform – PT23/00015) for the healthy control human specimens used in this study and the IDIPHISA Confocal Unit for the assistance with the multiplex Immunofluorescence panel.

Disclosure statement

EN reports research grants from Roche, Pfizer, BMS and Merck Serono; consulting fees from Roche, Bristol Myers Squibb, Merck Sharp Dohme, Merck-Serono, Sanofi, Pfizer, Lilly, Amgen, Janssen, Daiichi-Sankyo, Boehringer-Ingelheim, AstraZeneca, Takeda, Sanofi, Janssen, Pierre Fabre and Qiagen; honoraria for lectures from Roche, Bristol Myers Squibb, Merck Sharp Dohme, Sanofi, Pfizer, Lilly, Amgen, Janssen, Boehringer-Ingelheim, AstraZeneca, Takeda, Sanofi, Janssen and Qiagen; support for attending meetings from Takeda, Pfizer, Merck Sharp & Dohme, AstraZeneca and Roche and advisory board from Apollomics, Roche, Transgene and MSD. RGC reports research grants from BMS, consulting fees from Roche Novartis, BMS, MSD, AstraZeneca, Takeda, Janssen, GSK, Amgen, Sanofi, Boehringer and Lilly; payment or honoraria for lectures from Roche, Novartis, BMS, MSD, AstraZeneca, Takeda, Janssen, GSK, Amgen, Sanofi, Boehringer and Lilly; support for attending meetings from Roche, MSD, Janssen, AstraZeneca, Takeda and Pfizer; and fiduciary role in AstraZeneca. BM reports consulting fees from AstraZeneca and Amgen; payment or honoraria from Roche, Bristol Myers Squibb, and MSD; and support for attending meetings or travel from MSD and AstraZeneca. MD reports consulting fees from AstraZeneca, Bristol-Myers Squibb, MSD Oncology, Pharmamar, Pfizer, Roche and Takeda; payment or honoraria for lectures from AstraZeneca, Bristol-Myers Squibb, MSD Oncology, Pfizer, Roche, Takeda; and support for attending meetings from AstraZeneca, MSD Oncology, Pfizer and Takeda. AI reports payment or honoraria for lectures from Amgen, Bristol Myers Squibb, Regeneron, Roche and Takeda; support for attending meetings from Roche, Takeda, Pfizer and MSD; and participation on advisory board from AstraZeneca, Roche, Pfizer and Takeda. JdCC reports consulting fees from AstraZeneca, Bristol Myers Squibb, Roche, MSD, Boehringer, Janssen, Lilly, Sanofi, Takeda, Pfizer, and GSK; support for attending meeting or travel from AstraZeneca, MSD, and Roche; participation on advisory boards for AstraZeneca, Bristol Myers Squibb, Roche, MSD, Glaxo, Janssen, and Gilead; and speaker's bureau fees from AstraZeneca/MedImmune, Bristol-Myers Squibb, F. Hoffmann La Roche, Merck Sharpe & Dohme, MSD Oncology, Pfizer, and Janssen. MM reports grants from Roche and AstraZeneca; payment of honoraria from Roche, AstraZeneca, MSD, Pfizer, Helsinn, Cassen, Amgen, Janssen, Sanofi, Pierre Fabre, Bristol Myers Squibb, and Takeda; and support for attending meetings or travel from MSD, Roche, and AstraZeneca. AM-M reports consulting fees from AstraZeneca/MedImmune, Bristol-Myers Squibb, F. Hoffmann La Roche AG, Merck Sharp and Dohme, MSD Oncology, Pfizer, Janssen, Amgen and Fuchigec; honoraria for speaker's bureau from AstraZeneca/MedImmune, Bristol-Myers Squibb, F. Hoffmann La Roche AG, Merck Sharp and Dohme, MSD Oncology, Pfizer, Janssen and Amgen; payment for expert testimony from AstraZeneca/MedImmune, Bristol-Myers Squibb, F. Hoffmann La Roche AG, and MSD Oncology; support for attending meetings from AstraZeneca/MedImmune, Bristol-Myers Squibb, F. Hoffmann La Roche AG, Merck Sharp and Dohme, MSD Oncology, Pfizer, Janssen and Lilly, and participation on advisory board from AstraZeneca/MedImmune, Merck Sharp and Dohme, F. Hoffmann La Roche AG, Bristol-Myers Squibb, MSD Oncology, Pfizer, Janssen, Amgen and Fuchigec. AC-L reports honoraria for lectures from AstraZeneca, Roche, Pfizer, MSD, Takeda and BMS; payment for expert testimony from AstraZeneca; and support for attending meetings from AstraZeneca, Roche, MSD, Takeda and BMS. VC reports consulting fees from Roche, AstraZeneca, MSD, BMS, Takeda, Sanofi, Amgen, GSK, Boehringer Ingelheim and Janssen; honoraria for lectures from Roche, AstraZeneca, MSD, BMS, Takeda, Sanofi, Amgen, Pfizer, Janssen and Beigene; and support for attending meetings from AstraZeneca, Roche, MSD, Takeda and Janssen. MP reports MP reports grants, consulting fees and non-financial support from Bristol Myers Squibb, Roche, and AstraZeneca; and consulting fees from MSD and Takeda. All other authors declare no competing interests.

Funding

Work in the authors' laboratories was supported by "Instituto de Salud Carlos III" (ISCIII) PI19/01652 and PI22/01223 grants cofounded by European Regional Development Fund (ERDF), Bristol-Myers Squibb (BMS),

Ministry of Science and Innovation RTC2017-6502-1 'INmunoSIGHT', RTC2019-007359-1 'BLI-O', CPP2022-009545 'STRAGEN-IO', and European Union's Horizon 2020 research and innovation programme, CLARIFY 875160 grant, to MP. AC-B is supported by a "Miguel Servet" contract CP23/00044 by ISCIII and received an ISCIII project grant PI23/01054 both cofounded by European Union. CM-T is supported by Comunidad de Madrid PIPF-2022/SAL-GL-25283 contract granted to MP. MM-A is supported by Ayuda Predoctoral Asociación Española Contra el Cáncer (AECC) Madrid 2023 contract granted to MP. AnG-G was supported by Comunidad de Madrid and European social fund PEJ-2023-AI/SAL-GL-27634 contract, and now is supported by FI24/00270 predoctoral contract from ISCIII granted to AC-B.

ORCID

Belén Sierra Rodero  <http://orcid.org/0000-0003-0276-6088>
 Cristina Martínez-Toledo  <http://orcid.org/0000-0002-0663-0674>
 Ernest Nadal  <http://orcid.org/0000-0002-9674-5554>
 Marta Molina-Alejandre  <http://orcid.org/0000-0002-7167-610X>
 Rosario García Campelo  <http://orcid.org/0000-0003-2113-1504>
 Ángeles Gil-González  <http://orcid.org/0009-0005-2077-9191>
 Bartomeu Massuti  <http://orcid.org/0000-0002-6247-4493>
 Aránzazu García-Grande  <http://orcid.org/0000-0001-5737-8918>
 Manuel Dómine  <http://orcid.org/0000-0003-1634-9832>
 Amelia Insa  <http://orcid.org/0000-0002-3438-6170>
 Javier de Castro Carpeño  <http://orcid.org/0000-0002-3622-6306>
 Gerardo Huidobro Vence  <http://orcid.org/0000-0002-9167-6502>
 Margarita Majem  <http://orcid.org/0000-0002-9919-7485>
 Alex Martínez-Martí  <http://orcid.org/0000-0002-6714-9526>
 Diego Megias  <http://orcid.org/0000-0003-0755-0518>
 Daniel Lobato  <http://orcid.org/0009-0003-8118-4306>
 Ana Collazo-Lorduy  <http://orcid.org/0000-0003-4163-3392>
 Virginia Calvo  <http://orcid.org/0000-0002-3503-4847>
 Mariano Provencio  <http://orcid.org/0000-0001-6315-7919>
 Alberto Cruz-Bermúdez  <http://orcid.org/0000-0001-5136-7011>

Author contributions

BS-R: Formal analysis, investigation, visualization, methodology, writing – original draft, writing – review and editing. CM-T: Formal analysis, investigation, visualization, methodology, writing – review and editing. EN: Data curation, investigation, writing – review and editing. MM-A: Formal analysis, investigation, visualization, methodology, writing – review and editing. RGC: Data curation, investigation, writing – review and editing. MCa: Formal analysis, investigation, visualization, methodology, writing – review and editing. BM: Data curation, investigation, writing – review and editing. AG-G: Formal analysis, investigation, visualization, methodology, writing – review and editing. MD: Data curation, investigation, writing – review and editing. AI: Data curation, investigation, writing – review and editing. JdCC: Data curation, investigation, writing – review and editing. GHV: Data curation, investigation, writing – review and editing. MM: Data curation, investigation, writing – review and editing. AM-M: Data curation, investigation, writing – review and editing. DM: Investigation, methodology, writing – review and editing. DL: Investigation, methodology, writing – review and editing. AC-L: Data curation, investigation, writing – review and editing. VC: Data curation, investigation, writing – review and editing. MP: Conceptualization, resources, data curation, supervision, funding acquisition, investigation, project administration, writing – review and editing. AC-B: Conceptualization, resources, data curation, formal analysis, supervision, funding acquisition, investigation, visualization, methodology, writing original draft, project administration, writing – review and editing. AC-B is the guarantor of the study.

References

1. Siegel RL, Miller KD, Wagle NS, Jemal A. Cancer statistics, 2023. *CA Cancer J Clinicians*. 2023;73(1):17–48. doi: [10.3322/caac.21763](https://doi.org/10.3322/caac.21763).
2. Provencio M, Nadal E, Insa A, García-Campelo MR, Casal-Rubio J, Dómine M, Majem M, Rodríguez-Abreu D, Martínez-Martí A, De Castro Carpeño J, et al. Neoadjuvant chemotherapy and nivolumab in resectable non-small-cell lung cancer (NADIM): an open-label, multicentre, single-arm, phase 2 trial. *Lancet Oncol*. 2020;21(11):1413–1422. doi: [10.1016/S1470-2045\(20\)30453-8](https://doi.org/10.1016/S1470-2045(20)30453-8).
3. Provencio M, Nadal E, González-Larriba JL, Martínez-Martí A, Bernabé R, Bosch-Barrera J, Casal-Rubio J, Calvo V, Insa A, Ponce S, et al. Perioperative nivolumab and chemotherapy in stage III non-small-cell lung cancer. *N Engl J Med*. 2023;389(6):504–513. doi: [10.1056/NEJMoa2215530](https://doi.org/10.1056/NEJMoa2215530).
4. Cascone T, Awad MM, Spicer JD, He J, Lu S, Sepesi B, Tanaka F, Taube JM, Cornelissen R, Havel L, et al. Perioperative nivolumab in resectable lung cancer. *N Engl J Med*. 2024;390(19):1756–1769. doi: [10.1056/NEJMoa2311926](https://doi.org/10.1056/NEJMoa2311926).
5. Provencio M, Serna-Blasco R, Nadal E, Insa A, García-Campelo MR, Casal Rubio J, Dómine M, Majem M, Rodríguez-Abreu D, Martínez-Martí A, et al. Overall survival and biomarker analysis of neoadjuvant nivolumab plus chemotherapy in operable stage IIIA non-small-Cell lung cancer (NADIM phase II trial). *JCO JC* O2102660 (2022;40(25):2924–2933. doi: [10.1200/JCO.21.02660](https://doi.org/10.1200/JCO.21.02660).
6. Provencio M, Nadal E, Insa A, García Campelo R, Casal J, Dómine M, Massuti B, Majem M, Rodríguez-Abreu D, Martínez-Martí A, et al. Perioperative chemotherapy and nivolumab in non-small- cell lung cancer (NADIM): 5-year clinical outcomes from a multicentre, single-arm, phase 2 trial. *The Lancet Oncol*. 2024 (2024;25(11):1453–1464. doi: [10.1016/S1470-2045\(24\)00498-4](https://doi.org/10.1016/S1470-2045(24)00498-4).
7. Rosner S, Reuss JE, Zahurak M, Zhang J, Zeng Z, Taube J, Anagnostou V, Smith KN, Riemer J, Illei PB, et al. Five-year clinical outcomes after neoadjuvant nivolumab in resectable non-small cell lung cancer. *Clin Cancer Res*. 2023;29(4):705–710. doi: [10.1158/1078-0432.CCR-22-2994](https://doi.org/10.1158/1078-0432.CCR-22-2994).
8. Laza-Briviesca R, Cruz-Bermúdez A, Nadal E, Insa A, García-Campelo MDR, Huidobro G, Dómine M, Majem M, Rodríguez-Abreu D, Martínez-Martí A, et al. Blood biomarkers associated to complete pathological response on NSCLC patients treated with neoadjuvant chemoimmunotherapy included in NADIM clinical trial. *Clin Transl Med*. 2021;11(7). doi: [10.1002/ctm2.491](https://doi.org/10.1002/ctm2.491).
9. Sierra-Rodero B, Cruz-Bermúdez A, Nadal E, Garitaonandia Y, Insa A, Mosquera J, Casal-Rubio J, Dómine M, Majem M, Rodríguez-Abreu D, et al. Clinical and molecular parameters associated to pneumonitis development in non-small-cell lung cancer patients receiving chemoimmunotherapy from NADIM trial. *J Immunother Cancer*. 2021;9(8):e002804. doi: [10.1136/jitc-2021-002804](https://doi.org/10.1136/jitc-2021-002804).
10. Laumont M, Nelson BH. B cells in the tumor microenvironment: multi-faceted organizers, regulators, and effectors of anti-tumor immunity. *Cancer Cell*. 2023;41(3):466–489. doi: [10.1016/j.ccell.2023.02.017](https://doi.org/10.1016/j.ccell.2023.02.017).
11. Fridman WH, Meylan M, Pupier G, Calvez A, Hernandez I, Sautès-Fridman C. Tertiary lymphoid structures and B cells: an intratumoral immunity cycle. *Immunity*. 2023;56(10):2254–2269. doi: [10.1016/j.immuni.2023.08.009](https://doi.org/10.1016/j.immuni.2023.08.009).
12. Mei SQ, Liu J-Q, Huang Z-J, Luo W-C, Peng Y-L, Chen Z-H, Deng Y, Xu C-R, Zhou Q. Identification of a risk score model based on tertiary lymphoid structure-related genes for predicting immunotherapy efficacy in non-small cell lung cancer. *Thorac Cancer*. 2024;15(14):1119–1131. doi: [10.1111/1759-7714.15299](https://doi.org/10.1111/1759-7714.15299).
13. Ma J, Deng Y, Zhang M, Zhang Q. Spatial tertiary lymphoid structures imply response to anti-PD-1 plus anlotinib in advanced non-small cell lung cancer. *Immunology*. 2024;173(3):536–551. doi: [10.1111/imm.13841](https://doi.org/10.1111/imm.13841).
14. He M, He Q, Cai X, Liu J, Deng H, Li F, Zhong R, Lu Y, Peng H, Wu X, et al. Intratumoral tertiary lymphoid structure (TLS) maturation is influenced by draining lymph nodes of lung cancer. *J Immunother Cancer*. 2023;11(4):e005539. doi: [10.1136/jitc-2022-005539](https://doi.org/10.1136/jitc-2022-005539).
15. Sun X, Liu W, Sun L, Mo H, Feng Y, Wu X, Li C, Chen C, Li J, Xin Y, et al. Maturation and abundance of tertiary lymphoid structures are associated with the efficacy of neoadjuvant chemoimmunotherapy in resectable non-small cell lung cancer. *J Immunother Cancer*. 2022;10(11):e005531. doi: [10.1136/jitc-2022-005531](https://doi.org/10.1136/jitc-2022-005531).
16. Molina-Alejandre M, Perea F, Calvo V, Martínez-Toledo C, Nadal E, Sierra-Rodero B, Casarrubios M, Casal-Rubio J, Martínez-

- Martí A, Insa A, et al. Perioperative chemoimmunotherapy induces strong immune responses and long-term survival in patients with HLA class I-deficient non-small cell lung cancer. *J Immunother Cancer*. 2024;12(10):e009762. doi: [10.1136/jitc-2024-009762](https://doi.org/10.1136/jitc-2024-009762).
17. Sierra-Rodero B, Martínez-Toledo C, Molina-Alejandro M, Calvo V, Nadal E, Sureda BM, Campelo RG, Ojea CG, Martínez-Martí A, Gómez MD, et al. 187P tissue B-cell receptor repertoire as biomarker of complete pathological response in NSCLC patients treated with neoadjuvant chemoimmunotherapy (NADIM trials). *J Thorac Oncol*. 2023;18(4):S141–S142. doi: [10.1016/S1556-0864\(23\)00440-9](https://doi.org/10.1016/S1556-0864(23)00440-9).
 18. Xia L, Guo L, Kang J, Yang Y, Yao Y, Xia W, Sun R, Zhang S, Li W, Gao Y, et al. Predictable roles of peripheral IgM memory B cells for the responses to anti-PD-1 monotherapy against advanced non-small cell lung cancer. *Front Immunol*. 2021;12. doi: [10.3389/fimmu.2021.759217](https://doi.org/10.3389/fimmu.2021.759217).
 19. Barth DA, Stanzer S, Spiegelberg JA, Bauernhofer T, Absenger G, Szkandera J, Gerger A, Smolle MA, Hutterer GC, Ahyai SA. Patterns of peripheral blood B-Cell subtypes are associated with treatment response in patients treated with immune checkpoint inhibitors: a prospective longitudinal pan-cancer study. *Front Immunol*. 2022;13:1–10. doi: [10.3389/fimmu.2022.840207](https://doi.org/10.3389/fimmu.2022.840207).
 20. Carril-Ajuria L, Desnoyer A, Meylan M, Dalban C, Naigeon M, Cassard L, Vano Y, Rioux-Leclercq N, Chouaib S, Beuselinck B, et al. Baseline circulating unswitched memory B cells and B-cell related soluble factors are associated with overall survival in patients with clear cell renal cell carcinoma treated with nivolumab within the NIVOREN GETUG-AFU 26 study. *J Immunother Cancer*. 2022;10(5):e004885. doi: [10.1136/jitc-2022-004885](https://doi.org/10.1136/jitc-2022-004885).
 21. Van Gassen S, Callebaut B, Van Helden MJ, Lambrecht BN, Demeester P, Dhaene T, Saey Y. FlowSOM: using self-organizing maps for visualization and interpretation of cytometry data. *Cytometry Pt A*. 2015;87(7):636–645. doi: [10.1002/cyto.a.22625](https://doi.org/10.1002/cyto.a.22625).
 22. Fear VS, Forbes CA, Neeve SA, Fisher SA, Chee J, Waithman J, Ma SK, Lake R, Nowak AK, Creaney J, et al. Tumour draining lymph node-generated CD8 T cells play a role in controlling lung metastases after a primary tumour is removed but not when adjuvant immunotherapy is used. *Cancer Immunol Immun*. 2021;70(11):3249–3258. doi: [10.1007/s00262-021-02934-3](https://doi.org/10.1007/s00262-021-02934-3).
 23. Dammeijer F, van Gulijk M, Mulder EE, Lukkes M, Klaase L, van den Bosch T, van Nimwegen M, Lau SP, Latupeirissa K, Schetters S, et al. The PD-1/PD-L1-Checkpoint restrains T cell immunity in tumor-draining lymph nodes. *Cancer Cell*. 2020;38(5):685–700.e8. doi: [10.1016/j.ccell.2020.09.001](https://doi.org/10.1016/j.ccell.2020.09.001).
 24. Liu J, O'Donnell JS, Yan J, Madore J, Allen S, Smyth MJ, Teng MWL. Timing of neoadjuvant immunotherapy in relation to surgery is crucial for outcome. *Oncoimmunology*. 2019;8(5):1–12. doi: [10.1080/2162402X.2019.1581530](https://doi.org/10.1080/2162402X.2019.1581530).
 25. Inoue T, Kurosaki T, Kometani K, Ise W. Memory B cells. *Nat Rev Immunol*. 2015;15(3):149–159. doi: [10.1038/nri3802](https://doi.org/10.1038/nri3802).